JACS
JOURNAL OF THE AMERICAN CHEMICAL SOCIETY

Article

pubs.acs.org/JACS

Solvent and Temperature Probes of the Long-Range Electron-Transfer Step in Tyramine β-Monooxygenase: Demonstration of a Long-Range Proton-Coupled Electron-Transfer Mechanism

Hui Zhu,[‡,§] Monika Sommerhalter,[#] Andy K. L. Nguy,[†,§] and Judith P. Klinman*[,‡,†,§]

[‡]Department of Chemistry, [†]Department of Molecular and Cell Biology, and [§]California Institute for Quantitative Biosciences (QB3), University of California, Berkeley, California 94720-3220, United States

[#]Department of Chemistry and Biochemistry, California State University, East Bay, 25800 Carlos Bee Boulevard, Hayward, California 94542, United States

Supporting Information

ABSTRACT: Tyramine β-monooxygenase (TβM) belongs to a family of physiologically important dinuclear copper monooxygenases that function with a solvent-exposed active site. To accomplish each enzymatic turnover, an electron transfer (ET) must occur between two solvent-separated copper centers. In wild-type TβM, this event is too fast to be rate limiting. However, we have recently shown [Osborne, R. L.; et al. *Biochemistry* **2013**, *52*, 1179] that the Tyr216Ala variant of TβM leads to rate-limiting ET. In this study, we present a pH−rate profile study of Tyr216Ala, together with deuterium oxide solvent kinetic isotope effects (KIEs). A solvent KIE of 2 on k_{cat} is found in a region where k_{cat} is pH/pD independent. As a control, the variant Tyr216Trp, for which ET is not rate determining, displays a solvent KIE of unity. We conclude, therefore, that the observed solvent KIE arises from the rate-limiting ET step in the Tyr216Ala variant, and show how small solvent KIEs (ca. 2) can be fully accommodated from equilibrium effects within the Marcus equation. To gain insight into the role of the enzyme in the long-range ET step, a temperature dependence study was also pursued. The small enthalpic barrier of ET (E_a = 3.6 kcal/mol) implicates a significant entropic barrier, which is attributed to the requirement for extensive rearrangement of the inter-copper environment during PCET catalyzed by the Tyr216Ala variant. The data lead to the proposal of a distinct inter-domain pathway for PCET in the dinuclear copper monooxygenases.

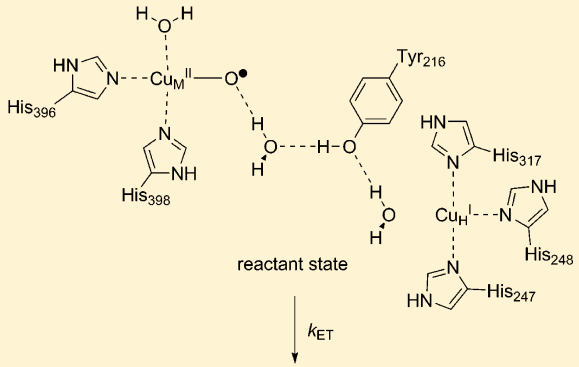

INTRODUCTION

The phenomenon of proton-coupled electron transfer (PCET) is an important process in chemistry and biology.[1−6] The electron transfer (ET) may be coupled with proton transfer (PT) as a way to balance charge or as a net reaction itself.[7] Compared to pure ET, the treatment of PCET becomes more complex because the mass of the proton is small enough that a significant quantum effect can be observed, but large enough that the quantum effect is limited to a small range (∼1 Å).[6] Thus, a long-range PCET will require mediators between the donor and acceptor to facilitate the transfer of the proton.[8,9] KIE studies have been performed on various PCET systems, including inorganic systems[10−13] and biological systems,[14−17] demonstrating that the range of KIE can vary from ∼2 (ref 10) to >100 (ref 16). Significant efforts have been made toward the theoretical treatment of PCET.[5,6]

As a continuous effort from our laboratory, the long-range ET process in the enzyme Tyramine β-monooxygenase (TβM) was studied. TβM belongs to a small family of eukaryotic enzymes containing two magnetically non-coupled copper centers at a distance of ca. 10 Å. These are designated Cu_M and Cu_H on the basis of their strictly conserved ligands (Met, His, His for Cu_M, and three His for Cu_H).[18−20] Enzymes within this family encompass dopamine β-monooxygenase (DβM) and peptidylglycine α-hydroxylating monooxygenase (PHM), and catalyze reactions of great physiological significance that result in the generation of the neurotransmitters octopamine and norepinephrine as well as peptide hormones.[18] The crystal structure has been solved for PHM showing the position of the two copper centers (Figure 1).[21] According to the proposed mechanism of the catalytic cycle (Scheme 1),[18,20,22,23] an ET between the two remote copper sites must take place in a highly efficient manner.[22] It has been previously proposed that the ET is facilitated by neither the substrate[24] nor the protein backbone,[25] occurring via the bulk water in the solvent cleft between the two coppers.[18]

Different research groups propose that the long-range ET is coupled with PT, but they disagree on the ET acceptor species.[22,23] The nature of the downstream step(s) has been

Received: December 4, 2014
Published: April 28, 2015

DOI: 10.1021/ja512388n
J. Am. Chem. Soc. 2015, 137, 5720−5729

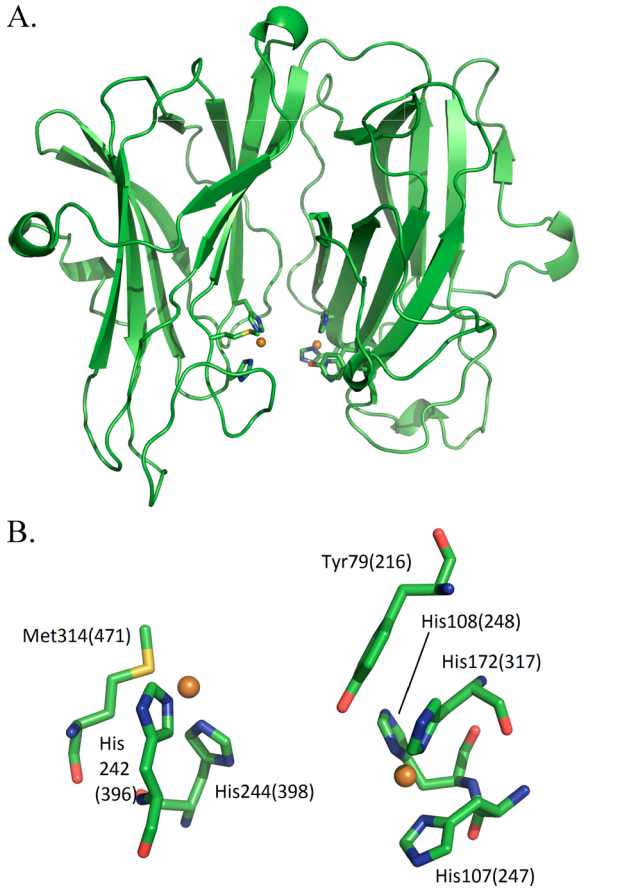

Figure 1. (A) X-ray crystal structure of the catalytic core of peptidylglycine α-hydroxylating monooxygenase (PDB: 1PHM). (B) The active site is enlarged to show the ligands coordinating to Cu_M (H242, H244, and M314) and Cu_H (H107, H108, and H172) and the conserved tyrosine (Y79 in PHM and Y216 in TβM) that is the focus of this study. Residue numbers are shown for PHM (without parentheses) and TβM (with parentheses).

Scheme 1. Proposed Mechanism for TβM[a]

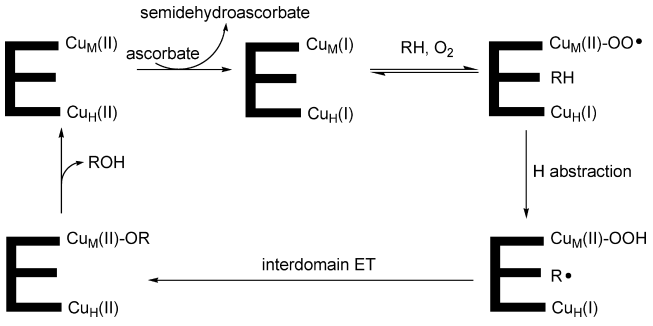

[a]This is a generic mechanism in which the ligands to copper and the movement of solvent protons are left ambiguous.

very difficult to access in the wild-type (WT) enzyme, as any step(s) that follow substrate activation are very fast.[20,26] While researchers agree that the second electron donor will be a reduced Cu(I) species at the Cu_H site, different copper−oxygen species have been proposed as the electron acceptor at the Cu_M site. Evans et al. proposed that a Cu_M(II) peroxide species accepts the electron from Cu_H(I), generating a Cu_M(II)-oxyl species that recombines with the substrate-derived radical to form an inner-sphere copper alkoxide species.[22] On the basis of density functional theory (DFT) calculations, Chen and Solomon proposed a pathway in which product (ROH) is generated prior to the ET step, with Cu_M(II)-oxyl serving as the electron acceptor species.[23] Recently, a novel rebound mechanism emerged during a Born−Oppenheimer molecular dynamics simulation; this third possibility involves an initially formed product hydroperoxide (ROOH) that undergoes a two-electron reductive cleavage using electrons from both Cu_H(I) and Cu_M(I).[27] The first and third mechanisms predict the generation of an inner-sphere copper-alkoxide species, while the second mechanism leads to the initial generation of an outer-sphere complex of hydroxylated product with copper hydroxide.

A common feature of all the proposed ET pathways is the requirement to mobilize protons, making the prediction that the long-range ET will be a PCET process. As in all PCET processes, the timing of such coupling is of great interest, in particular, whether the PT occurs before, during, or after the ET step. In addition to the conservation of the ligands to Cu_M and Cu_H, all enzymes of this class contain a tyrosine (Tyr) observed to π-stack with one of the His ligands at the Cu_H site.[19,26]

Recently, we have characterized a variant of TβM at this Tyr (Tyr216Ala) that displays an altered kinetic mechanism, in which the intersite ET has become rate-determining under conditions of substrate saturation.[26] This conclusion arose from a detailed study of the impact of substrate deuteration on k_{cat} and k_{cat}/K_m for WT,[20] Tyr216Trp (where Trp is tryptophan), Tyr216Ile (where Ile is isoleucine), and Tyr216Ala (where Ala is alanine). An important finding was that the large KIE on k_{cat}/K_m approaches the intrinsic KIE of the chemical step (ca. 12)[28,29] in the case of Tyr216Ala, indicating that the substrate off rate must be significantly faster than the chemical step. Extensive analysis[26] led to the conclusion of a similar increase in the off rate of product, for Tyr216Ala, requiring a kinetically significant ET step that is not present in WT or other variants (cf. Table S1). This enables the direct study of the ET process in Tyr216Ala TβM by kinetic means.

In this study, we apply solvent and temperature probes (solvent kinetic isotope effect (KIE), pH profile, proton inventory, and temperature dependence of k_{cat}) to exploit the unique kinetic properties of the Tyr216Ala variant, putting forth a kinetic pathway and mechanism for this variant of TβM. The data are analyzed within a new theoretical context for rationalizing small solvent KIEs[10,11,13,15] in PCET processes.

EXPERIMENTAL SECTION

Materials. *Drosophila* Schneider 2 (S2) cells and *Drosophila* Expression System were purchased from Invitrogen. Blasticidin S-HCl was purchased from Sigma-Aldrich. Insect Xpress growth medium was acquired from Lonza. Anion-exchange chromatography medium was purchased from Sigma-Aldrich. The HiPrep 26/60 Sephacryl S-200 HR size exclusion column was from GE Healthcare. Assay reagents were obtained from Sigma-Aldrich or Fisher Scientific. Methanol (Fisher Optima grade, 99.9%) and purified water (to a resistivity of 18.2 MΩ·cm at 25 °C using a Milli-Q Gradient ultrapure water purification system) were used to prepare mobile-phase solvents for HPLC.

Protein Expression and Purification. Tyr216Ala TβM that lacks a His tag was expressed in *Drosophila* S2 cells, collected and purified as described previously.[19,30] Briefly, the secretion of protein was induced by 0.5 mM $CuSO_4$ for 3 days. Protein purification involved Q-sepharose anion exchange and size-exclusion chromatography. Pure fractions (single banded, as determined by SDS-PAGE) were pooled and concentrated, and protein concentration was determined by UV absorbance at 280 nm. The molecular weight and extinction

DOI: 10.1021/ja512388n
J. Am. Chem. Soc. 2015, 137, 5720−5729

coefficient of Tyr216Ala TβM are MW = 67 664.7 Da, ε_{280} = 96 230 $M^{-1}\cdot cm^{-1}$.[26]

Enzyme Kinetic Assays. Enzymatic reactions were performed in a jacketed chamber with the water bath temperature controlled at 35 °C. The stocks of potassium phosphate buffers at different pH values were made by mixing 1.0 M KH_2PO_4 solution and 1.0 M K_2HPO_4 solution, and the pH was monitored by a pH electrode calibrated with standard pH solutions on the same day. The potassium phosphate buffers in heavy water were made in a similar fashion except the pD of the solution is determined by adding 0.4 to the pH value displayed by the electrode.[31] For mixed light water and heavy water solutions, eq 1 is used for correction of the pH value monitored by the glass electrode:[31]

$$(\Delta pH)_n = 0.076n^2 + 0.3314n \quad (1)$$

where n is the mole fraction of heavy water. The reaction solutions were 2 mL in total volume, and contained 100 mM KCl, 50 μM to 4 mM tyramine, 10 mM sodium ascorbate, 2 μM $CuSO_4$ (in a 2-fold excess to saturate the enzyme), 100 μg/mL catalase, and potassium phosphate buffer of various pH values; the ionic strength was maintained as 150 mM by varying the concentration of the buffer without introducing additional salts. The reaction solutions were saturated with pure oxygen gas for 10 min before the addition of 2 μL of 100−200 μM enzyme solution, leading to a final concentration of 1040 μM, ca. 5 times the K_m for O_2 in H_2O (206 μM inferred from ref 26). In the context of a D_2O-independent k_{cat}/K_m for substrate (after correcting for the impact of solvent on pK_a perturbation, see below), we have made a similar assumption regarding k_{cat}/K_m for oxygen. This implies a reduction in the K_m for oxygen in D_2O relative to the K_m value of 206 μM in H_2O at pH 6.0. Reactions were quenched at 1−10 min time points by transferring 150−200 μL aliquots to 3 μL of 70% $HClO_4$. The concentrations of octopamine generated were determined by HPLC (see below). The reaction rates were obtained by a linear regression of the product generation versus time. The activities of enzymes prepared on different days were normalized by performing a standard rate assay containing 1 mM tyramine at pH 6.0. The data were fitted to the form of the Michaelis−Menten equation that includes a term for the substrate inhibition (eq 2).The value of K_i was found to change very little across the pH

$$v = \frac{k_{cat}[E]_0[S]}{K_m + [S](1 + [S]/K_i)} \quad (2)$$

range studied and after substitution of H_2O by D_2O. An average value of K_i = 1.9 mM was thus used in all fittings of pH profile and solvent KIE studies in order to reduce the uncertainty in k_{cat}.

Product Analysis by HPLC. The precision of the data presented has required an assay distinct from the O_2 depletion monitored in some previous studies,[20,26] as this gives rise to a large nonenzymatic background O_2 consumption at pH > 7.0. The far more laborious HPLC-based assay was, therefore, employed. This involved an Alltech Adsorbosphere reversed phase C-18 column (Grace Discovery Sciences, 4.6 × 250 mm) attached to a Beckman-Coulter system Gold HPLC equipped with a system Gold autosampler and a system Gold 168 detector to monitor the absorbance at 224 nm. Separation of tyramine and octopamine from other assay components was achieved using a mobile phase of 5 mM acetic acid, 0.6 mM heptanesulfonic acid, and 15% methanol, pH adjusted to 5.8 with 1 M NaOH, at a flow rate of 1.1 mL/min; under these conditions, octopamine eluted at a retention time of 8−9 min. The area under the octopamine peak was integrated, and the octopamine concentration was calculated using a standard curve generated with a series of octopamine stock solutions in a concentration range of 1−200 μM.[20] Previously, it has been shown that no octopamine forms in the absence of enzyme (data not shown).

RESULTS

The pH Profile and Solvent KIE of Tyr216Ala TβM. The Tyr216Ala TβM-catalyzed conversion of tyramine into octopamine was monitored at elevated oxygen (>1 mM) as a function of varying tyramine concentration in H_2O and D_2O at varying pL values (Figures S1−S6). First- and second-order rate constants, k_{cat} and $k_{cat}/K_{m,Tyr}$, and the resulting solvent KIEs are summarized in Table 1. The pH profiles for k_{cat} of Tyr216Ala TβM in H_2O and D_2O are presented in Figure 2A, and the solvent KIEs at each pH are presented in Figure 2C. In the pH region of 5.5−7.5, the k_{cat} in H_2O does not change appreciably. A small increase of ca. 47% is observed from pH 7.5 to pH 8.0, and could indicate the onset of an ionization with a pK_a higher than 8.0. This feature is absent for k_{cat} in D_2O. The secondary effect which might arise above pH 7.5 was not investigated further. The remaining data indicate an increase in the solvent KIE between pL 5.5 and 7.5, to yield maximum values of 1.98 ± 0.16 (pL 7.0) and 2.06 ± 0.11 (pL 7.5). Alternatively, using the average k_{cat} values in H_2O of 0.91 ± 0.02 (pH 5.5−7.5) and in D_2O of 0.53 ± 0.05 (pD 5.5−8.0), the solvent KIE is estimated as 1.71 ± 0.17. The KIEs measured for k_{cat} are significantly greater than what would be caused by the viscosity difference of D_2O and H_2O, which are reported to be ≤1.2 (refs 32−34).

Distinct from k_{cat}, the second-order rate constant ($k_{cat}/K_{m,Tyr}$), displays a bell shape pH dependence in H_2O, as presented in Figure 2B. The data were fitted by least-squares method according to eq 3, which gives C = 4.8 ± 0.8, pK_A =

$$k = \frac{C}{1 + 10^{pK_A - pH} + 10^{pH - pK_B}} \quad (3)$$

6.0 ± 0.2, pK_B = 7.6 ± 0.2 for rate constants in H_2O, and C = 5.7 ± 1.3, pK_A = 6.6 ± 0.3, pK_B = 9 ± 3 for rate constants in D_2O. The maximum rate constant C for reaction in H_2O and D_2O is the same within error, indicating little or no effect of solvent deuteration on $k_{cat}/K_{m,Tyr}$. The estimated second ionization, pK_B, for the reaction in D_2O is too uncertain for

Table 1. Kinetic Parameters Measured for Tyr216Ala TβM at Different pL in H_2O and D_2O[a]

	H_2O		D_2O			
pL	k_{cat} (s^{-1})	k_{cat}/K_m (mM^{-1} s^{-1})	k_{cat} (s^{-1})	k_{cat}/K_m (mM^{-1} s^{-1})	$^Dk_{cat}$	$^D(k_{cat}/K_m)$
5.5	0.924 ± 0.087	1.15 ± 0.09	0.563 ± 0.079	0.768 ± 0.110	1.64 ± 0.28	1.50 ± 0.24
6.0	0.906 ± 0.035	3.04 ± 0.36	0.704 ± 0.047	1.18 ± 0.11	1.29 ± 0.10	2.58 ± 0.39
6.5	0.976 ± 0.032	4.05 ± 0.22	0.653 ± 0.026	2.36 ± 0.16	1.50 ± 0.08	1.72 ± 0.15
7.0	0.878 ± 0.039	2.98 ± 0.26	0.444 ± 0.029	4.60 ± 0.09	1.98 ± 0.16	0.647 ± 0.057
7.5	0.882 ± 0.028	2.46 ± 0.19	0.427 ± 0.019	9.04 ± 2.50	2.06 ± 0.11	0.272 ± 0.078
8.0	1.30 ± 0.08	1.46 ± 0.07	0.417 ± 0.023	4.98 ± 0.71	3.12 ± 0.25	0.293 ± 0.044

[a]Measured at 35 °C, 1 mM O_2. Fitted with nonlinear least-square method, using k_{cat} and k_{cat}/K_m as independent parameters and a fixed K_i of 1.9 mM. Errors are presented as standard errors from the fitting of eq 2.

DOI: 10.1021/ja512388n
J. Am. Chem. Soc. 2015, 137, 5720−5729

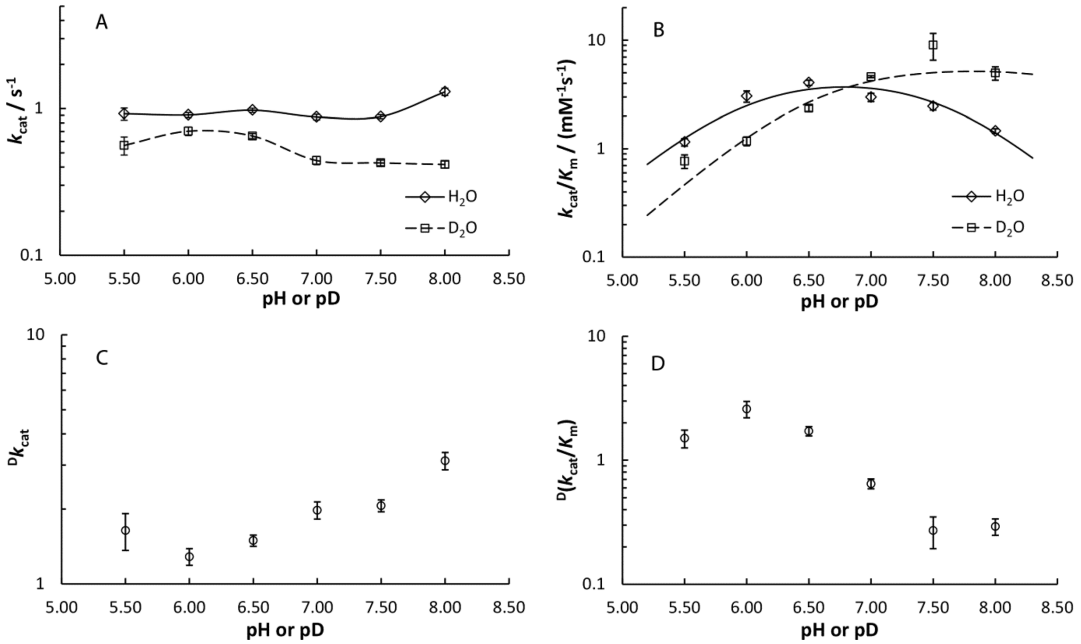

Figure 2. Solvent isotope effects for Tyr216Ala TβM. (A,B) pH profiles in H_2O (blue) vs D_2O (red). (C,D) Isotope effects on $^{D}k_{cat}$ and $^{D}(k_{cat}/K_m)$, respectively. Error bars are presented as standard error, or 68% confidence interval.

any comparisons, but the first ionization, pK_A, is significantly larger in D_2O than H_2O. This difference falls in the range of D_2O-induced shifts on pK_a values of proteins[31] as one would expect. The trend in $^{D}(k_{cat}/K_m)$, which changes from normal to inverse across the pL range (Figure 2D) is, thus, attributed to the solvent induced perturbation in pK_A.

To establish whether the solvent KIE on k_{cat} is a unique property of Tyr216Ala TβM, we performed a control experiment. In a previous investigation of a series of amino acid substitutions at Tyr216, it was found that inter-domain ET is the rate-determining step for Tyr216Ala, in marked contrast to Tyr216Trp, which resembles the WT with regard to substrate isotope effects and rate-limiting steps.[26] As a control experiment, solvent KIEs were, therefore, measured for Tyr216Trp. Indeed, the solvent KIEs measured are 1.05 ± 0.18 at pL 6.0 and 0.86 ± 0.17 at pL 7.5, which are close to unity and different from the solvent KIEs of Tyr216Ala (Figure 3). An inverse KIE appears on k_{cat}/K_m at pL 7.5, which is likely a result of an ionization process similar to the Tyr216Ala mutant as discussed above. These results show that the KIE of 2 observed for Tyr216Ala variant is a unique property of its rate-limiting step.

Proton Inventory Experiment of Tyr216Ala TβM. In order to determine the number of protons involved in the ET step, a proton inventory[31] experiment was performed at pL 7.5, and the results are presented together with three different models (eqs S1−S3, Figure 4). At each D_2O level, full Michaelis−Menten kinetics were performed by varying the concentration of tyramine, and fitted to eq 2. The data show a continuous decrease in k_{cat} with increasing deuterium content of the solvent, as expected when the major impact of solvent on a kinetic phenomenon arises from a kinetically significant PT process. We tentatively suggest a single site PT, but we cannot eliminate the possible involvement of more protons. The small amplitude of the isotope effect together with the size of the error envelopes in these discontinuous kinetic assays renders it difficult to discriminate between the possible models presented in Figure 4.

Temperature Dependence of k_{cat} for Tyr216Ala TβM. Michaelis−Menten kinetic curves were measured in H_2O at different temperatures ranging from 288 to 308 K (Table 2). The kinetic parameters are fitted according to eq 2. The rate constant of ET (k_{ET}) at each temperature is equated to k_{cat}, assuming that the previous demonstration of rate-limiting ET at 308 K remains true at all temperatures.[26] Fitting the data with the Arrhenius equation (eq 4) gives E_a = 3.6 ± 0.7 kcal·mol^{-1}

$$k = A\, e^{-E_a/RT} \tag{4}$$

and $\ln(A/s^{-1})$ = 5.6 ± 1.2. The remarkably small temperature dependence is further discussed in the following section.

As pointed out by several reviewers, comparative experiments in D_2O have the potential to distinguish whether solvent KIEs arise from the activation energy (E_a) or the pre-exponential factor (A). However, with our current method for activity assays of TβM, the error associated with the parameters would be too large to draw decisive conclusion, and this additional approach was not pursued.

DISCUSSION

Link of PT to ET in Tyr216Ala TβM. While an extensive study of the pH dependence of WT TβM has not been pursued, the properties of Tyr216Trp reveal a ca. 2-fold reduction in k_{cat} between pH 6.0 and 7.5 (Figure 3). This behavior resembles the pH dependence of DβM,[35] which shows a biphasic dependence on pH, with a pK_a of 5.39 ± 0.25, and a k_{cat} that is reduced ca. 5 times at the higher pH. The pH profile of PHM[36] also shows that the enzyme has an active phase flanked by two inactive phases characterized by pK_a values of 5.9 ± 0.1 and 8.1 ± 0.1. These results differ from Tyr216Ala TβM, which shows a pH-independent k_{cat} in the similar pH range (Figure 2). The pH independence of k_{cat} for a variant of TβM where ET has become rate limiting indicates two facts: first, there are no relevant protonations or deprotonations that alter the rate of ET, and second, the ET itself is

DOI: 10.1021/ja512388n
J. Am. Chem. Soc. 2015, 137, 5720−5729

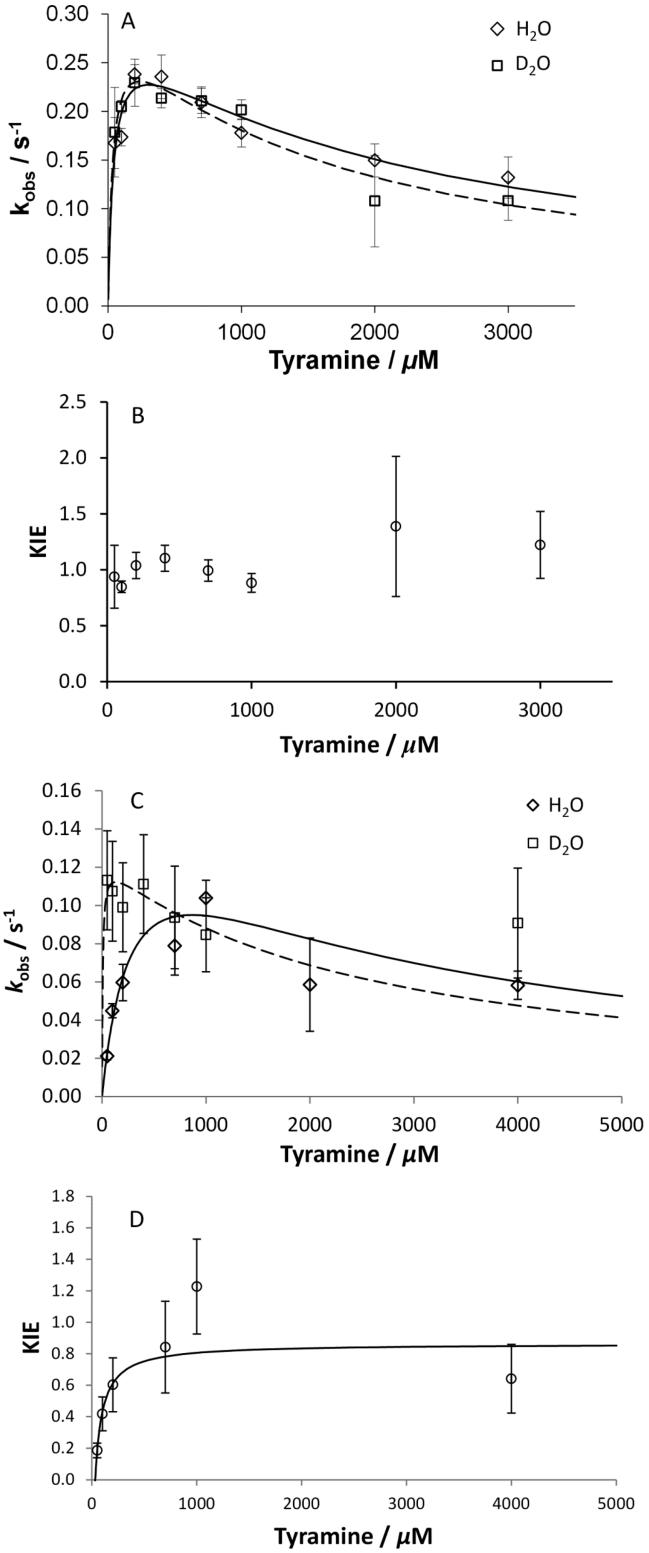

Figure 3. Apparent rate constant and KIE of Tyr216Trp TβM at various concentrations of tyramine, (A,B) at pL 6.0 and (C,D) at pL 7.5. Error bars are presented as standard error, or 68% confidence interval.

likely independent of any *net* protonation or deprotonation. At the same time, the rate of ET expresses a solvent KIE, from which we conclude that an inter-domain ET is coupled to an inter-domain proton(s).

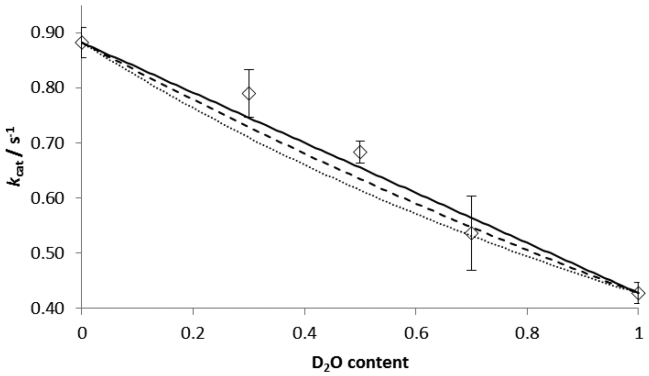

Figure 4. Proton inventory experiment of Tyr216Ala TβM at pL 7.5. The solid lines represent a single PT (solid line), two-site transfer with the same KIE (dashed line), and an infinite site transfer model (dotted line). Errors are presented as $\pm 1\sigma$, or 68% confidence interval.

Table 2. Kinetic Parameters Measured for Tyr216Ala TβM at Different Temperatures[a]

T (K)	k_{ET} (s^{-1})
288	0.456 ± 0.065
293	0.554 ± 0.063
298	0.579 ± 0.059
303	0.590 ± 0.045
308	0.739 ± 0.100

[a]Measured at pH 7.5, with 1 mM O_2.

Rationale of Observed KIE. The relatively small size of the solvent KIE suggests that the PCET is *not* a fully concerted EPT barrier-crossing mechanism, which can be approximated as a net hydrogen atom transfer. Cárdenas et al.[37] optimized a transition state for a fully concerted EPT in PHM by DFT calculation. Using an active-site model that incorporates a water molecule at Cu_H, together with two more water molecules that provide a bridge to the Cu_M site, three hydrogens were found to be transferred simultaneously in the TS. Unfortunately, the authors did not calculate a KIE on the basis of their TS structure. Notably, in another system expected to undergo a multiproton transfer, namely the carbonic anhydrase reaction, a semiclassical transition-state theory treatment for the multiproton transfer calculated a KIE of 18.0,[38] contrasting with the small experimental KIE of 3−4 (refs 39,40) that is more similar to Tyr216Ala TβM. We consider it likely that a water chain facilitates the PCET process in TβM, and that the small KIE makes a hydrogen atom transfer unlikely. Here we will discuss two theoretical frameworks developed by Jortner[41] and Hammes-Schiffer[6] that are capable of rationalizing small solvent KIEs for PCET processes, and present a third approach based on Marcus theory[42] that explains the KIE on the basis of a change in the reaction driving force (ΔG^0).

Jortner[41] has developed a formulism to calculate KIEs on the basis of nuclear tunneling effects. This approach focuses on the small nuclear displacement accompanying the ET event, and attributes the KIE to the different wave packets of the isotopically labeled nuclei. It should be noted that the difference in zero-point energies of isotopologues was initially omitted (i.e., the change in ΔG^0 for isotopologues was assumed to be zero). This formula has successfully reproduced a number of experimental results, including the magnitude of a $H_2{}^{18}O$ solvent KIE on ET between liganded metal ions[11] and the trend of the ^{18}O KIE in glucose oxidase reconstituted with flavin

DOI: 10.1021/ja512388n
J. Am. Chem. Soc. 2015, 137, 5720−5729

cofactors of different driving force.[43] In ref 11, the experimental solvent D_2O KIE (ca. 2) was compatible with the impact of D_2O on measured redox potentials. These authors "corrected" the measured KIEs for equilibrium solvent D_2O effects, focusing their analysis on the heavy-atom ^{18}O effects. In fact, they suggested that almost all of the H/D KIE was likely due to differences in ΔG^0 between isotopologues; however, no explicit theory was presented.

Hammes-Schiffer has developed a theory to explain the rate and KIE of PCET, which employs quantum treatments on both the transferred electron and proton.[6] Specifically, the PT is treated as electronically adiabatic and vibrationally nonadiabatic; i.e., the transfer rate is calculated as a weighted sum of PT of all of the possible pairs of different vibrational states for the donor and acceptor. This theory has successfully reproduced the large KIE and the small temperature dependence of soybean lipoxygenase[44,45] as well as small KIEs for proton−electron self-exchange of iron bi-imidazoline complexes.[12,46] In the latter case, the KIE is reported as 2.3 ± 0.3 at 324 K,[12] and it is shown that the observed KIE can be reproduced by allowing vibrationally nonadiabatic proton/deuteron transfer.[46] As a result, the KIE is attenuated by a quantum treatment, which could seem "puzzling".[47] However, the effect can be rationalized by an increased contribution for deuterium of reactant wave function overlap to excited-state vibrational modes of the product.

While a full quantum treatment is capable of reproducing small KIEs, a validated semiclassical framework could offer unique mechanistic insights into PCET. As we show below, it is possible to explain the data for TβM by treating the movement of the electron according to Marcus theory and the movement of the transferred proton as a semiclassical equilibrium process that impacts the ΔG^0 term within $\Delta G^{\ddagger}$.

Use of Marcus Theory To Infer Possible PCET Pathways on Tyr216Ala TβM. The Marcus theory elegantly connects the free energy barrier of an ET event with the driving force (ΔG^0) and the intrinsic reorganization energy (λ) of the heavy-atom environment, according to eq 5.

$$\Delta G^{\ddagger} = \frac{\lambda}{4}\left(1 + \frac{\Delta G^0}{\lambda}\right)^2 \tag{5}$$

Equation 6 is the expression for a non-adiabatic ET rate according to Marcus theory under the high-temperature limit:[48]

$$k_{ET} = \frac{2\pi}{\hbar}(H_{AB})^2 \frac{1}{\sqrt{4\pi\lambda k_B T}}\, e^{-\Delta G^{\ddagger}/k_B T} \tag{6}$$

where $\hbar$ is the reduced Planck's constant, k_B is Boltzmann's constant, and H_{AB} is the electronic coupling factor that includes the distance effect. Under the high-temperature limit, it is generally assumed that k_BT is larger than the excitation energy of relevant vibrational modes, leading to classical behavior in this domain. While this assumption is legitimate for solvent modes below 100 cm^{-1}, it is obvious that a k_BT of room temperature is much smaller than the excitation energy of stretching modes of covalent bonds between heavy atom and hydrogen, and hydrogen bonds between an H-bond donor and acceptor, which are in the range of 2500−3500 cm^{-1}.

Herein we describe an approach that treats the high-frequency vibrational states of exchangeable O−H bonds semiclassically,[43] showing that the observed KIE can be modeled from a change of ΔG^0 in ground-state force constants for the reactants and products of ET. It is reasonable to assume that the overall shape of the parabola of a potential energy surface, representing the participation of a large number of heavy atoms (including the copper ions in TβM), is unchanged by isotopic substitution, and that the major impact of this perturbation will be on the vibrational modes of the substrate and product states. According to our model, the rate of ET is dominated by the environmental reorganization term (λ), while the KIE arises solely from changes in ΔG^0. As previously discussed,[43] incorporation of ground-state vibrational states into the Marcus theory can be accomplished by vertical shifts in the energies at the bottom of the parabolas representing the initial and final states.

If we notate the H/D isotope effect on $\Delta G^{\ddagger}$, ΔG^0, and λ as $\Delta\Delta G^{\ddagger}$, $\Delta\Delta G^0$, and $\Delta\lambda$, and assume that they are small changes, we can formulate the Marcus theory in a differentiated form:

$$\Delta\Delta G^{\ddagger} = \left(\frac{\partial\Delta G^{\ddagger}}{\partial\Delta G^0}\right)\Delta\Delta G^0 + \left(\frac{\partial\Delta G^{\ddagger}}{\partial\lambda}\right)\Delta\lambda \tag{7}$$

where

$$\frac{\partial\Delta G^{\ddagger}}{\partial\Delta G^0} = \frac{\Delta G^0 + \lambda}{2\lambda} \tag{8}$$

$$\frac{\partial\Delta G^{\ddagger}}{\partial\lambda} = -\frac{1}{4}\left(\frac{\Delta G^0}{\lambda}\right)^2 + \frac{1}{4} \tag{9}$$

The incorporation of a deuterium KIE into the Marcus theory has been discussed before by Marcus.[42] In the earlier treatment, the assumption was made that the KIE relies solely on a perturbation of the reorganization energy. However, since the reorganization process for the long-range ET in TβM involves many atoms moving coordinatively, we considered it unlikely that the change of reduced mass upon solvent deuteration would be appreciable, making $\Delta\lambda \approx 0$. We therefore proceeded to analyze the KIE on $\Delta G^{\ddagger}$ as arising from the equilibrium isotope effect on ΔG^0, showing how this approach can provide both a rationale for TβM behavior and further insight into its PCET mechanism.

$$\Delta\Delta G^{\ddagger} = \left(\frac{\Delta G^0 + \lambda}{2\lambda}\right)\Delta\Delta G^0 \tag{10}$$

The sensitivity of $\Delta\Delta G^{\ddagger}$ to $\Delta\Delta G^0$ depends on the values of ΔG^0 and λ. The only scenario in which $\Delta\Delta G^{\ddagger} = 0$ is when $\Delta G^0 = -\lambda$, a highly unlikely scenario for TβM and the majority of reactions involving PCET processes. Under the combined condition of $\Delta G^0 \geq 0$ and $\lambda \geq \Delta G^0$, $\Delta\Delta G^{\ddagger}$ is sensitive to $\Delta\Delta G^0$, with the limit $\Delta\Delta G^{\ddagger} = \Delta\Delta G^0$ when $\Delta G^0 = \lambda$ and $\Delta\Delta G^{\ddagger} = {}^1/_2\,\Delta\Delta G^0$ when $\Delta G^0 = 0$.

Following from eq 10, the relationship between the measured KIE and the impact of solvent D_2O on the barrier height ($\Delta\Delta G^{\ddagger}$) is given by eq 11.

$$\mathrm{KIE} = e^{-\Delta\Delta G^{\ddagger}/RT} \tag{11}$$

Combining eq 10 with eq 11, we can estimate that a KIE of 2.0 corresponds to a $\Delta\Delta G^0$ of ca 0.4−0.8 kcal/mol. To demonstrate this point clearly, numerical fittings are provided in the Supporting Information using explicit values for ΔG^0 and λ. We attribute the change in driving force, $\Delta\Delta G^0$, to the impact of

DOI: 10.1021/ja512388n
J. Am. Chem. Soc. 2015, 137, 5720−5729

deuteration on the zero-point energy difference (ΔΔZPE) between the reactant state and species that forms from ET. In order to generate a positive ΔΔZPE, it is expected that the intermediate resulting from ET will have proton vibrational modes with smaller total force constants than for the reactant.[49]

In our application of eqs 10 and 11 to TβM, we have, for illustrative purposes, focused on the mechanism advanced by Solomon and co-workers (cf. Scheme 2A).[23] As shown, PCET occurs between Cu_H and an oxygen free radical at Cu_M, converting one molecule of H_2O into two Cu-OH centers. As documented,[26] the long-range ET is slow and rate-limiting for Tyr216Ala. We considered the possibility that the reductant ascorbate might intercept the ET reaction, by interacting directly with the radical at Cu_M. However, we argue that this is unlikely, because the reduction of the highly reactive Cu_M(II)-O$^\bullet$ is expected to take place prior to the loss of enzyme-bound product. In a previous study,[20] it was shown that competitive inhibition occurs between tyramine and ascorbate in the reduction of Cu_M(II), which, by extension to the product complex, would greatly reduce or prevent any reaction of Cu_M(II)-O$^\bullet$ with exogenous reductant.

According to the PCET of Scheme 2A, two O−H stretching modes and one H−O−H bending mode from H_2O are lost, forming two O−H stretching modes, two Cu−O−H in-plane bending modes and two Cu−O−H out-of-plane bending/disformation modes from the two Cu−OH product centers. Accordingly, the expected net frequency change of hydrogen vibrational mode(s) can be approximated from the IR properties of H_2O and $Cu(OH)_2$. The vibrational wavenumbers of liquid phase water have been recorded as 3375 cm^{-1} (O−H stretch, two modes) and 1635 cm^{-1} (H−O−H bending).[50] The IR spectrum of $Cu(OH)_2$ in aqueous solution is not available in the literature. Instead, it has been recorded in a solid argon matrix trapped form at 10 K,[51] and assigned an O−H stretch, Cu−O−H in-plane bending, and Cu−O−H out-of-plane bending/disformation at 3635, 720, and 469 cm^{-1}, respectively. These values are also cited by the NIST database.[50] The frequency of the measured O−H stretching is likely free of the impact of hydrogen-bonding, which would decrease its frequency. For example, the O−H stretching mode of water in liquid phase is ∼330 cm^{-1} less than in the gas phase. Therefore, in the solvent-exposed active site of TβM, the O−H stretching frequency of Cu−OH species can be approximated as 3305 cm^{-1}, after correction for hydrogen-bonding effects. Compared to the liquid phase vibrational wavenumbers of water, a net 603 cm^{-1} *increase* of the bending and stretching vibrational modes is estimated for the mechanism under consideration (Scheme 2A). This value implies an inverse (<1) KIE, rather than the normal KIE of 2.0 we observed. On this basis, we rule out a single-step mechanism in which the reactant proceeds directly to the product state in which PT is complete (Scheme 2A). Instead, we propose *a transient reorganization that weakens the hydrogen-bonded network between Cu_H and Cu_M as the key process in facilitating inter-copper electron tunneling.* Immediately following ET, the resulting metastable hydrogen-bonded intermediate is expected to decay rapidly to the final product (Scheme 2).

In the absence of a more quantitative estimate of driving force and reorganization energy, it is difficult to specify the exact intermediate generated in the rate-determining ET process. Nonetheless, from the above analysis of the experimental

Scheme 2. Proposed Mechanism for the PCET Step

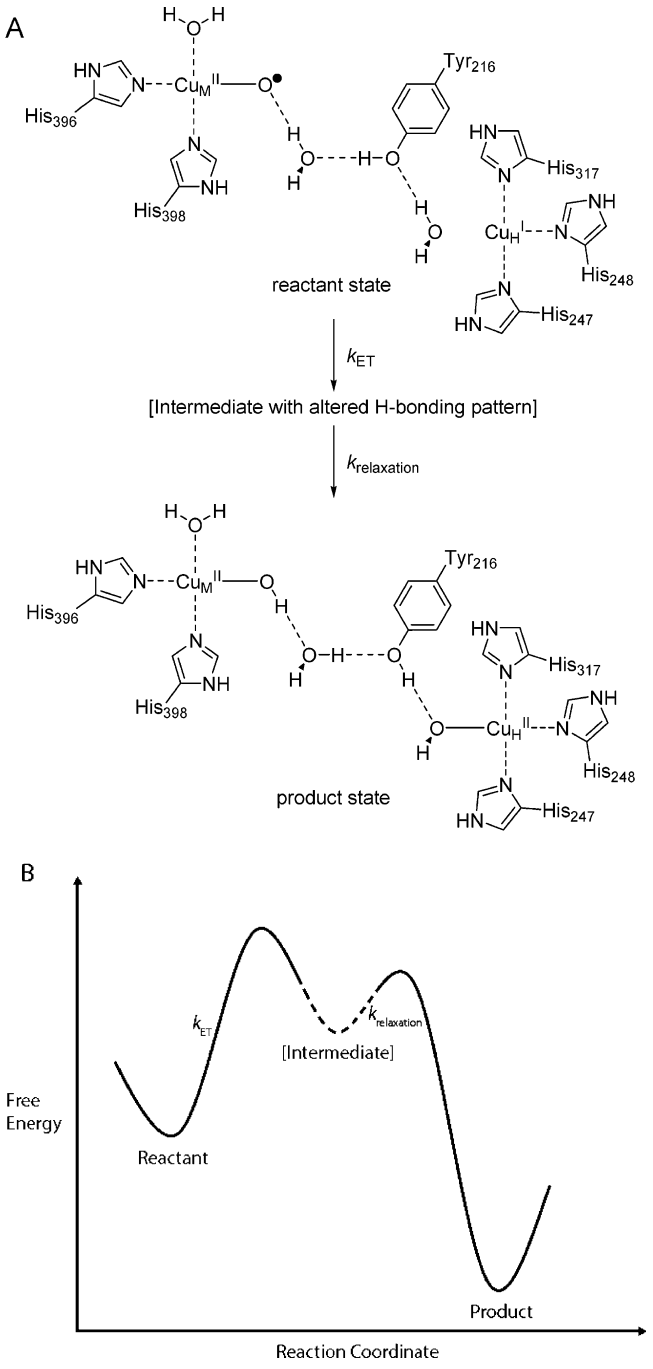

solvent KIE, we propose that the ET in TβM, as well as other enzyme systems characterized by small solvent KIEs,[52] may arise as the result of small, transient adjustments in the hydrogen-bonding network connecting the donor and acceptor sites. This will involve, by necessity, a reduction in the force constants for the O−H stretching and bending modes, producing an activated state from which the electron can flow from donor to acceptor. In the case of WT TβM, the OH group of Tyr216 is proposed to serve as the key element in structuring the local hydrogen-bonding, making proton coupled ET in WT much faster than the Tyr216 variants. Given our inability to directly interrogate the ET step in WT, we do not know the size of its solvent KIE. It is reasonable to assume, though by no means is it proven, that a similar mechanism and

DOI: 10.1021/ja512388n
J. Am. Chem. Soc. 2015, 137, 5720−5729

solvent KIE operate for WT as for Tyr216Ala. The large reduction in rate for ET in the latter,[26] may arise from an entropic penalty that arises from the substitution of Tyr216 by a solvent water (see below). In the case of Tyr216Trp TβM, the retention of a rate-limiting step similar to that of WT is likely the combined result of a reduction in the rate for product release[26] together with the capacity of the indole side chain to enter into H-bonding with active-site water(s).

A report has recently appeared,[13] describing the reaction of an inorganic copper(II) superoxide complex with the phenolic O−H of a series of 2,6-di-*tert*-butylphenol derivatives at very low temperatures. The authors observe a linear correlation between the logarithm of the reaction rate of H-abstraction from para-substituted 2,6-di-*tert*-butylphenols and the redox potential of these phenol H-donors. KIEs for the para-MeO- and para-Me-substituted substrates are 11 and 4 at 183 K. Significant changes on the redox potential upon deuteration on the hydroxyl group are also seen for both the MeO and Me substrates with reported increases of 0.059 and 0.086 V, respectively. Moreover, the deuterated substrates can be fitted on the same linear free energy relationship of rate and redox potential as for substitution effects (Figure 6, bottom line, ref 13). The observation of a large impact of deuteration on *both* the equilibrium redox potentials and kinetic constants strongly suggests that isotopic equilibrium effects are at play that impact the rate of ET. We propose that this recent model study of Cu(II) superoxide reactivity can be understood in the context of the theory developed herein for the long-range PCET of TβM. In the published work, the authors ruled out a rate-limiting ET followed by fast PT mechanism with the statement "no KIE would be observed in contrast to our experimental observations" (note 39 in ref 13). However, the attribution of an isotope effect to $\Delta\Delta G^0$ offers an alternate interpretation of their study. We suggest that the theory presented here should be considered, in general, when attempting to rationalize the origin of relatively small KIEs in PCET reactions.

Temperature Dependence of ET Rate. To gain deeper insight into the boundaries of the reorganization energy λ and driving force ΔG^0 for a PCET that generates an intermediate with altered H-bonding properties (Scheme 2A), a temperature study was performed with Tyr216Ala TβM, and analyzed using the nonadiabatic Marcus equation (eq 6).[48,53]

In order to fit eq 6, an estimation of the electronic coupling term H_{AB} is needed. H_{AB} has the unit of energy, is pathway dependent, and empirically decays exponentially with distance

$$H_{AB}(r) = H_{AB}(r_0)\, e^{-(\beta/2)(r-r_0)} \quad (12)$$

(eq 12).[54] In eq 12, r is the distance between donor and acceptor in Å, r_0 is the close contact van der Waals distance, and β is the decay factor of the ET medium. Beratan and co-workers[55] have found that structured water can be a superior mediator of ET compared to protein matrix and bulk water. The solvent-filled cleft of TβM possesses a similar distance to the interprotein ET studied by Beratan,[55] which falls into the "structured water" region with an accompanying H_{AB} of 0.011 kcal·mol^{-1}.

The two parameters (ΔG^0 and λ) that contribute to the thermal barrier cannot be determined simultaneously. On the basis of the previous discussion that the ΔG^0 should be $\geq$0, we fixed ΔG^0 at three values, 0, 5, and 10 kcal·mol^{-1} to calculate λ.

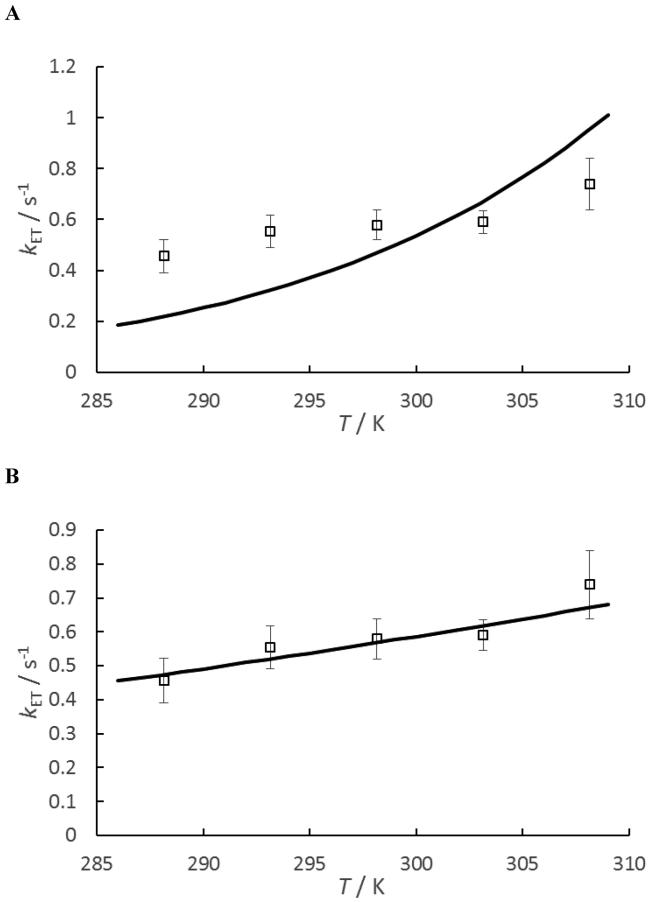

Figure 5. Plot of fitted temperature dependence of ET rate. (A) The experimental data cannot be fit from enthalpic terms alone. (B) Incorporating an entropic term into either ΔG^0 or λ (Table 3) allows the data to be fit quite well. The curves in panels A and B are equivalent for ΔG^0 = 0, 5, or 10 kcal/mol.

However, initial fitting of λ showed that the fitted curve overestimates the temperature dependence of k_{ET} yielding an inferior fit (Table S2, Figure 5A). We attribute this phenomenon to the neglect of an entropic term in either ΔG^0 or λ. Therefore, a second fitting effort that breaks down either ΔG^0 or λ to their enthalpic and entropic components was performed. In this fitting, ΔG^0 has been fixed at three values, 0, 5, and 10 kcal·mol^{-1}, and the entropic component assigned entirely to either ΔG^0 or λ. The experimental data are well-fitted in either case at each of the fixed ΔG^0 values (Table 3, Figure 5B).

Although it was not possible to obtain exact λ and ΔG^0 values from the temperature dependence study, it can be inferred that there is a significant entropy term in the driving force or reorganization energy. This result implies that, compared to the ET reactant state, the barrier for creating the intermediate H-bonded structure capable of supporting ET requires considerable restructuring of the active-site (water) molecules. This may not be surprising, given the absence of the conserved tyrosine in Tyr216Ala. While there are examples of free radical intermediates involving conserved active-site tyrosines,[17] there is neither an absolute dependence of TβM on Tyr216 nor any evidence for radical generation at this site. We propose that Tyr216 in WT TβM preorganizes the active site in a way that reduces the entropic barrier to $\Delta G^{\ddagger}$. The

DOI: 10.1021/ja512388n
J. Am. Chem. Soc. 2015, 137, 5720−5729

Table 3. Fitted Parameters of Temperature Dependence of ET Rate at Each Fixed Driving Force Value

ΔG^0 (kcal·mol^{-1})	ΔH^0 (kcal·mol^{-1})	$-T\Delta S^0$ [a] (kcal·mol^{-1})	λ (kcal·mol^{-1})	enthalpic component of λ (kcal·mol^{-1})	entropic component of λ [a] (kcal·mol^{-1})	χ^2 [b]
0[c]	−22.6	22.6	58.7	58.7	0[c]	1.27
5[c]	−15.6	20.6	48.4	48.4	0[c]	1.27
10[c]	−8.0	18.0	36.5	36.5	0[c]	1.27
0[c]	0[c]	0[c]	52.6	14.3	38.3	1.26
5[c]	5[c]	0[c]	42.3	3.4	38.9	1.26
10[c]	10[c]	0[c]	30.0	−13.0	43.0	1.27

[a] $-T\Delta S^0$ and entropic component of λ are calculated using T = 298 K. [b] χ^2 is the goodness of fit, defined as $\chi^2 = \sum((O - E)^2/\sigma^2)$, where, for each data point, O is the observed value, E is the predicted value from the fitting, and σ is the error. $H_{AB}(r)$ is estimated as 0.011 kcal·mol^{-1}. [c] These terms are fixed in the fitting.

latter is certainly expected to be one of the major factors supporting rapid PCET in native TβM.

CONCLUSION

The solvent kinetic isotope effect is reported for Tyr216Ala TβM, which has previously been concluded to be limited by a long-range inter-domain electron-transfer process under conditions of substrate saturation. The solvent KIE on k_{cat} of ~2.0 can be explained by a model of water-assisted proton-coupled electron transfer. The formation of an altered hydrogen-bonded intermediate is proposed to facilitate a rate-determining ET, and the magnitude of KIE can be rationalized by such an effect using the non-adiabatic Marcus theory with isotopic changes to the vibrational zero-point energy. This proposal is also supported by the small temperature dependence of the ET rate, which implies the contribution of a large negative entropy change in the driving force (or reorganization energy). Concomitant with a significant increase in the rate constant for release of product from enzyme,[26] the origin of the rate-limiting PCET in Tyr216Ala is attributed to a disruption of a highly structured hydrogen-bonded network/pathway centered on Tyr216 in the wild-type enzyme.

ASSOCIATED CONTENT

Supporting Information

Equations S1−S3 for the models of proton inventory, numerical examples for solvent KIE, Tables S1 and S2, and Figures S1−S6. This material is available free of charge via the Internet at http://pubs.acs.org.

AUTHOR INFORMATION

Corresponding Author

*klinman@berkeley.edu

Notes

The authors declare no competing financial interest.

ACKNOWLEDGMENTS

We thank Dr. Agostino Migliore, Prof. David Beratan (Duke University), and Prof. Sharon Hammes-Schiffer (University of Illinois) for their helpful suggestions and discussions. M.S. is grateful for a sabbatical year granted by California State University, East Bay. This work is supported by a grant from the NIH to J.P.K. (GM025765).

REFERENCES

(1) Huynh, M. H. V.; Meyer, T. J. *Chem. Rev.* **2007**, *107*, 5004.
(2) Reece, S. Y.; Nocera, D. G. *Annu. Rev. Biochem.* **2009**, *78*, 673.
(3) Dempsey, J. L.; Winkler, J. R.; Gray, H. B. *Chem. Rev.* **2010**, *110*, 7024.
(4) Weinberg, D. R.; Gagliardi, C. J.; Hull, J. F.; Murphy, C. F.; Kent, C. A.; Westlake, B. C.; Paul, A.; Ess, D. H.; McCafferty, D. G.; Meyer, T. J. *Chem. Rev.* **2012**, *112*, 4016.
(5) Migliore, A.; Polizzi, N. F.; Therien, M. J.; Beratan, D. N. *Chem. Rev.* **2014**, *114*, 3381.
(6) Hammes-Schiffer, S.; Stuchebrukhov, A. A. *Chem. Rev.* **2010**, *110*, 6939.
(7) Belevich, I.; Verkhovsky, M. I.; Wikstrom, M. *Nature* **2006**, *440*, 829.
(8) Costentin, C.; Robert, M.; Saveant, J. M.; Tard, C. *Angew. Chem., Int. Ed.* **2010**, *49*, 3803.
(9) Stubbe, J.; Nocera, D. G.; Yee, C. S.; Chang, M. C. Y. *Chem. Rev.* **2003**, *103*, 2167.
(10) Hudis, J.; Dodson, R. W. *J. Am. Chem. Soc.* **1956**, *78*, 911.
(11) Guarr, T.; Buhks, E.; McLendon, G. *J. Am. Chem. Soc.* **1983**, *105*, 3763.
(12) Roth, J. P.; Lovell, S.; Mayer, J. M. *J. Am. Chem. Soc.* **2000**, *122*, 5486.
(13) Lee, J. Y.; Peterson, R. L.; Ohkubo, K.; Garcia-Bosch, I.; Himes, R. A.; Woertink, J.; Moore, C. D.; Solomon, E. I.; Fukuzumi, S.; Karlin, K. D. *J. Am. Chem. Soc.* **2014**, *136*, 9925.
(14) Yoon, S.; Lippard, S. J. *Inorg. Chem.* **2006**, *45*, 5438.
(15) Jenson, D. L.; Evans, A.; Barry, B. A. *J. Phys. Chem. B* **2007**, *111*, 12599.
(16) Hu, S. S.; Sharma, S. C.; Scouras, A. D.; Soudackov, A. V.; Carr, C. A. M.; Hammes-Schiffer, S.; Alber, T.; Klinman, J. P. *J. Am. Chem. Soc.* **2014**, *136*, 8157.
(17) Smirnov, V. V.; Roth, J. P. *J. Biol. Inorg. Chem.* **2014**, *19*, 1137.
(18) Klinman, J. P. *J. Biol. Chem.* **2006**, *281*, 3013.
(19) Gray, E. E.; Small, S. N.; McGuirl, M. A. *Protein Express. Purif.* **2006**, *47*, 162.
(20) Hess, C. R.; McGuirl, M. M.; Klinman, J. P. *J. Biol. Chem.* **2008**, *283*, 3042.
(21) Prigge, S. T.; Kolhekar, A. S.; Eipper, B. A.; Mains, R. E.; Amzel, L. M. *Science* **1997**, *278*, 1300.
(22) Evans, J. P.; Ahn, K.; Klinman, J. P. *J. Biol. Chem.* **2003**, *278*, 49691.
(23) Chen, P.; Solomon, E. I. *J. Am. Chem. Soc.* **2004**, *126*, 4991.
(24) Francisco, W. A.; Wille, G.; Smith, A. J.; Merkler, D. J.; Klinman, J. P. *J. Am. Chem. Soc.* **2004**, *126*, 13168.
(25) Bell, J.; El Meskini, R.; D'Amato, D.; Mains, R. E.; Eipper, B. A. *Biochemistry* **2003**, *42*, 7133.
(26) Osborne, R. L.; Zhu, H.; Iavarone, A. T.; Blackburn, N. J.; Klinman, J. P. *Biochemistry* **2013**, *52*, 1179.
(27) Melia, C.; Ferrer, S.; Rezac, J.; Parisel, O.; Reinaud, O.; Moliner, V.; de la Lande, A. *Chem.—Eur. J.* **2013**, *19*, 17328.
(28) Francisco, W. A.; Merkler, D. J.; Blackburn, N. J.; Klinman, J. P. *Biochemistry* **1998**, *37*, 8244.
(29) Miller, S. M.; Klinman, J. P. *Biochemistry* **1985**, *24*, 2114.
(30) Hess, C. R.; Klinman, J. P.; Blackburn, N. J. *J. Biol. Inorg. Chem.* **2010**, *15*, 1195.
(31) Schowen, K. B.; Schowen, R. L. *Methods Enzymol.* **1982**, *87*, 551.
(32) Gadda, G.; Fitzpatrick, P. F. *FEBS Lett.* **2013**, *587*, 2785.
(33) Spies, M. A.; Toney, M. D. *Biochemistry* **2003**, *42*, 5099.

DOI: 10.1021/ja512388n
J. Am. Chem. Soc. 2015, 137, 5720−5729

(34) Smith, M. D.; Collins, R. A. *Proc. Natl. Acad. Sci. U.S.A.* **2007**, *104*, 5818.
(35) Ahn, N.; Klinman, J. P. *Biochemistry* **1983**, *22*, 3096.
(36) Bauman, A. T.; Jaron, S.; Yukl, E. T.; Burchfiel, J. R.; Blackburn, N. J. *Biochemistry* **2006**, *45*, 11140.
(37) Cárdenas, D. J.; Cuerva, J. M.; Alias, M.; Bunuel, E.; Campana, A. G. *Chem.—Eur. J.* **2011**, *17*, 8318.
(38) Smedarchina, Z.; Siebrand, W.; Fernandez-Ramos, A.; Cui, Q. *J. Am. Chem. Soc.* **2003**, *125*, 243.
(39) Steiner, H.; Jonsson, B. H.; Lindskog, S. *Eur. J. Biochem.* **1975**, *59*, 253.
(40) Pocker, Y.; Bjorkquist, D. W. *Biochemistry* **1977**, *16*, 5698.
(41) Buhks, E.; Bixon, M.; Jortner, J.; Navon, G. *J. Phys. Chem.* **1981**, *85*, 3759.
(42) Marcus, R. A. *J. Phys. Chem.* **1968**, *72*, 891.
(43) Roth, J. P.; Wincek, R.; Nodet, G.; Edmondson, D. E.; McIntire, W. S.; Klinman, J. P. *J. Am. Chem. Soc.* **2004**, *126*, 15120.
(44) Knapp, M. J.; Rickert, K.; Klinman, J. P. *J. Am. Chem. Soc.* **2002**, *124*, 3865.
(45) Hatcher, E.; Soudackov, A. V.; Hammes-Schiffer, S. *J. Am. Chem. Soc.* **2004**, *126*, 5763.
(46) Iordanova, N.; Decornez, H.; Hammes-Schiffer, S. *J. Am. Chem. Soc.* **2001**, *123*, 3723.
(47) Marcus, R. A. *Philos. Trans. R. Soc. B* **2006**, *361*, 1445.
(48) Marcus, R. A.; Sutin, N. *Biochim. Biophys. Acta* **1985**, *811*, 265.
(49) Bigeleisen, J.; Wolfsberg, M. *Adv. Chem. Phys.* **1958**, *1*, 15.
(50) Kirilovsky, D.; Roncel, M.; Boussac, A.; Wilson, A.; Zurita, J. L.; Ducruet, J. M.; Bottin, H.; Sugiura, M.; Ortega, J. M.; Rutherford, A. W. *J. Biol. Chem.* **2004**, *279*, 52869.
(51) Wang, X. F.; Andrews, L. *Inorg. Chem.* **2005**, *44*, 9076.
(52) For example, one key step of photosystem II, the reduction of a tyrosine radical intermediate, has been found to have a solvent KIE of 2 (ref 15). The authors attributed the KIE to either a CPET mechanism or a PT equilibrium followed by a rate-limiting ET.
(53) Davidson, V. L. *Biochemistry* **2000**, *39*, 4924.
(54) Beratan, D. N.; Betts, J. N.; Onuchic, J. N. *Science* **1991**, *252*, 1285.
(55) Lin, J. P.; Balabin, I. A.; Beratan, D. N. *Science* **2005**, *310*, 1311.

DOI: 10.1021/ja512388n
J. Am. Chem. Soc. 2015, 137, 5720−5729